Deep Learning Networks for Channel Estimation in Underwater OFDM Systems

A Project Report

submitted by

Abhiram (17EC117)

B.Ajay (17EC210)

Sunnyhith Yadlapalli (17EC154)

under the guidance of

B.Nagavel

in partial fulfilment of the requirements

for the award of the degree of

BACHELOR OF TECHNOLOGY

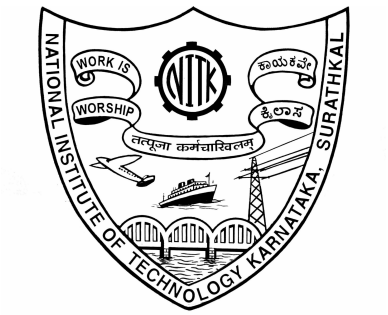

DEPARTMENT OF ELECTRONICS AND COMMUNICATION ENGINEERING

NATIONAL INSTITUTE OF TECHNOLOGY KARNATAKA

SURATHKAL, MANGALORE - 575025

November 30, 2020

ABSTRACT

Orthogonal frequency division multiplexing (OFDM) provides a promising modulation technique for underwater acoustic (UWA) communication systems. It is indispensable to obtain channel state information for channel estimation to handle the various channel distortions and interferences. However, the conventional channel estimation methods such as least square (LS), minimum mean square error (MMSE) and back propagation neural network (BPNN) cannot be directly applied to UWA-OFDM systems, since complicated multipath channels may cause a serious decline in performance estimation. To address the issue, two types of channel estimators based on deep neural networks (DNNs) are proposed with a novel training strategy in this paper. The proposed DNN models are trained with the received pilot symbols and the correct channel impulse responses in the training process, and then the estimated channel impulse responses are offered by the proposed DNN models in the working process. The experimental results demonstrate that the proposed methods outperform LS, BPNN algorithms and are comparable to the MMSE algorithm in respect to bit error rate and normalized mean square error. Meanwhile, there is no requirement of prior statistics information about channel autocorrelation matrix and noise variance for our proposals to estimate channels in UWA-OFDM systems, which is superior to the MMSE algorithm.In this project BEllHOP ray model is used to design under water channel making it nearer to the real time environment.

TABLE OF CONTENTS

LIST OF FIGURES

CHAPTER 1
Introduction

Underwater acoustic (UWA) channels are usually regarded as one of the most difficult communication mediums.Compared to general wireless communication scenarios,UWA channels suffer from a variety of environmental factors,including temperature, salinity, pressure, limited bandwidth,multipath effect, Doppler shift, transmission loss, ocean noise and so on. These complicated UWA environment places higher requirements and greater challenges to achieve high-efficiency and reliable transmissions for wireless communication. More recently, the orthogonal frequency division multiplexing (OFDM) technique has been adopted to UWA communications, due to its excellent performance in resisting inter symbol interference (ISI) and reducing multipath fading effect. As a multicarrier system, OFDM divides the channel bandwidth into a large number of orthogonal narrowband subcarriers, such that each individual subcarrier which occupies only a small bandwidth can be modulated with a conventional modulation scheme at a low data rate,maintaining the total data rates equal to a single carrier system with the same bandwidth. This feature guarantees OFDM systems with high-speed transmission and high spectrum efficiency for wireless communication over UWA multipath channels.Channel estimation is critical to the performance of UWA-OFDM systems. Since the transmission signal is generally distorted by the channel characteristics when through multipath channels, the channel impulse response (CIR) must be estimated to recover the transmitted signal coherently at the receiver. To this end, some pilot symbols are usually sent together with the data subcarriers to obtain the CIR for channel estimation, where the pilot symbols are also priori known to the receiver. With the help of these pilot symbols, estimation techniques can then be utilized to evaluate the significant information of CIR for UWA-OFDM systems, such as least squares (LS) algorithm, minimum mean square error (MMSE) algorithm.

1.1 Problem definition

The major problem in applying OFDM to underwater channels is the motion-induced Doppler distortion which creates non-uniform frequency offset in a wideband acoustic signal. Previous work on this problem has focused on two approaches: adaptive synchronization, which requires little overhead but relies on coherence between adjacent OFDM blocks, and non-adaptive synchronization, which requires null subcarriers to gain robustness to fast channel variations. Here, we extend the approach by coupling it with channel estimation in the time domain (impulse response). The motivation for doing so is the possibility to perform channel sparsing. Channel impulse response is often shorter than an OFDM block, and can thus be represented by fewer than K coefficients that it takes to represent its transfer function on the K subcarriers. A certain number L¡K coefficients of the time-domain response can be efficiently estimated using L equally-spaced data symbols, a method used. We suggest a slight but important modification to this method to make it applicable to a general underwater channel, where the strongest signal arrival may not be the first one. Sparsing is implemented in an optimal manner simply by magnitude truncation of the time-domain channel coefficients. When the channel is truly sparse, performance improvement results from eliminating the unnecessary noise present in the full-size (overparametrized) channel estimate.

1.2 Previous work

In recent years, there have been a growing interest in artificial neural network (ANN), for its strong ability to learn from the environments in supervised as well as unsupervised ways, mimicking the human brain with numerous interconnected neurons. This advantage makes it highly suitable for solving complex nonlinear problems, including image recognition, signal processing, computer vision, robotics and so on. In particular, many types of neural networks have been successfully applied to the problem of channel estimation in wireless communications.A type of radial basis function (RBF) neural network was proposed for channel estimation in pilot symbol aided OFDM systems, the structure of which was designed by the pilot pattern to effectively restore the channel response. Reference developed an ANN channel estimation technique for OFDM systems without assistance of pilot symbols over Rayleigh fading channels, increasing the bandwidth efficiency compared to pilot-based estimation techniques. For multiple input multiple output-orthogonal frequency division multiplexing (MIMO-OFDM) systems, ANN-based channel estimators were presented to estimate channel effect using comb-type pilot arrangement and trained continuously by feedback symbols over mobile communications channels.Among many network models, one of the most commonly used is back propagation neural network (BPNN) with three layers of neurons, generally proposed to estimate the channel characteristics of OFDM systems . In BPNNs were expanded into space time coded MIMO-OFDM systems and orthogonal frequency division multiplexing-interleave division multiple access (OFDM-IDMA) systems for estimating the channel coefficients. Furthermore,combined the BPNN with genetic algorithm to improve the estimation performance and convergence rate, which is usually used to search for reliable solutions to optimization problems.

These provide a feasible guidance for the application of DNN to complex UWA communications, but the obstacles of these DNN models in are that a massive number of storage resources are needed to preserve the network parameters, and a high latency of running time will occur during the application process. Different from these DNN models, we attempt to design a properly sized neural network architecture to save storage resources and running time while satisfying the desired performance requirements for channel estimation in UWA-OFDM systems. in these works.

1.3 Motivation

Nowadays most of the research works concentrate on using acoustic sensor nodes for underwater communication. Acoustic methodologies are the most widely used in underwater communication. Communication in underwater by multipath propagation gives reflection and refraction. The velocity of sound under water is 1500 meter per second. Due to this multipath propagation do not provide efficiency in communication. The various modes of communication applied in the earlier approach shows the growth of underwater communication due to the range of the communication. After ultrasound communication nowadays acoustic communication provides better communication range. According to the human activities expansion the inter-medium communication is also getting increased. Than other communication systems underwater communication is growing continuously and speedily.

1.4 Overview

Underwater wireless communication techniques have played the most important role in the exploration of oceans and other aquatic environments. Underwater acoustic (UWA) communication faces a lot of hurdles such as environmental characteristics, variety of noises, temperature, pressure, salinity, etc which makes the UWA channel unique. UWA channel modeling is the most demanding task due to its time-varying property and due to its double dispersion property resulting in severe multipath spread and time variation. Accurate estimation and tracking of channel state information (CSI) are required for receiver design and channel capacity analysis in an underwater environment. The goal of this study is to provide a comprehensive survey on channel estimation of the latest researches in the field of UWA communication. The previous works are summarized, reviewed and compared according to their years of publication. This paper provides an overview on the channel model, methods, and algorithms for channel estimation and equalization in an underwater environment. It also includes a journey of channel estimation from time-varying UWA multipath model towards the estimation of a multipath underwater channel in the Multiple-input Multiple-output Orthogonal Frequency Division Multiplexing (MIMO OFDM) environment.

CHAPTER 2

Description

2.1 UWA-OFDM SYSTEM MODEL

A schematic diagram of the UWA-OFDM system model is illuminated in Fig.2.1. Suppose that the binary data sequence is firstly encoded and mapped with quadrature amplitude modulation (QAM) modulation schemes.

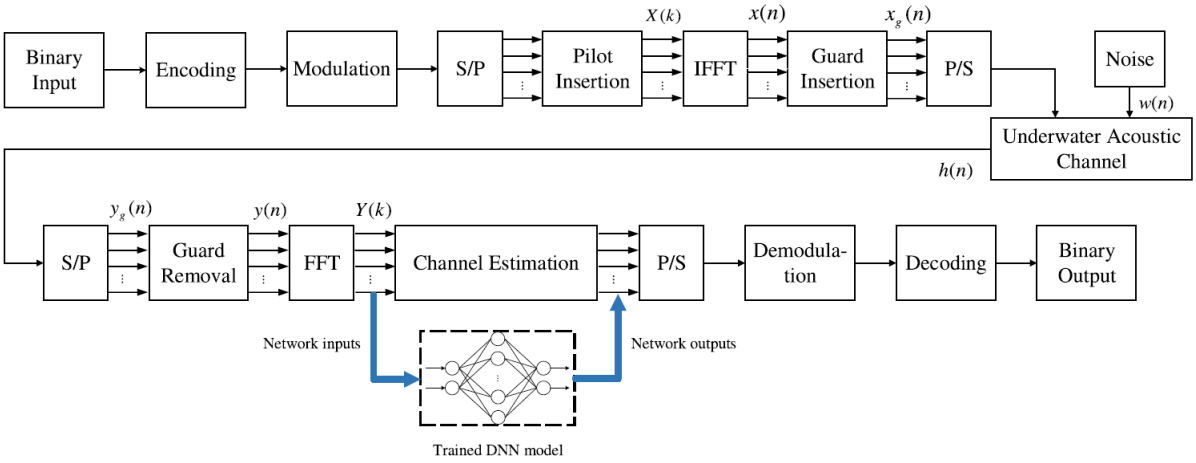

Figure 2.1: Block diagram of UWA-OFDM system model

The modulated signal is converted from serial to parallel ones, and the pilot tones are inserted to estimate the CIR of the channel model. In the UWA-OFDM system, the parallel data are transformed by inverse fast Fourier transform (IFFT) with N orthogonal narrowband subcarriers. The time domain signal x(n) is obtained from the frequency domain signals X(k) as follows:

$$x(n) = (\frac{1}{N}) \sum_{k=0}^{N-1} X(k) e^{j\frac{2\pi}{N}nk} \tag{2.1}$$

After IFFT, the N parallel subcarriers are converted to a serial bitstream and the cyclic prefix samples are inserted as guard intervals to alleviate the ISI. So the time-domain transmitted signal including cyclic prefix can be represented as follows:

$$x_g(n) = \begin{cases} x(N+n) & \text{n} = -N_g, -N_g+1, ... -1 \\ x(n) & \text{n} = 0, 1, ...N-1 \end{cases} \tag{2.2}$$

where n_g is the length of cyclic prefix samples. It means that the last n_g samples of x(n) are duplicated as cyclic prefix and inserted to the beginning of this symbol, resulting the signal $x_g(n)$ with length of N + n_g.

After through the underwater acoustic channel, the received signal $y_g(n)$ is given by:

$$y_g(n) = x_g(n) \otimes h(n) + w(n), -N_g < n < N-1 \tag{2.3}$$

where the operator $\otimes$ corresponds to the circular convolution and w(n) is the additive white Gaussian noise (AWGN) with zero-mean. h(n) is the channel impulse response that can be represented as follows:

$$h(n) = \sum_{i=0}^{r-1} h_i \delta(n - \tau_i) \tag{2.4}$$

where δ is impulse response, r is the number of multipaths, h_i and $_i$ are the discrete complex gain and time delay of the i-th tap.

In the receiver, the received signal is split into parallel subcarriers and the cyclic prefix is removed out. Then the time-domain signal y(n) is transformed to frequency-domain signal Y(k) by fast Fourier transform (FFT) operations as follows:

$$Y(k) = (\frac{1}{N}) \sum_{k=0}^{N-1} y(n) e^{-j\frac{2\pi}{N}nk}, k = 0, 1, ..., N-1 \tag{2.5}$$

thus under the assumption that the ISI is completely eliminated, the received signal can be formulated as:

$$Y(k) = X(k)H(k) + W(k), k = 0, 1, ..., N - 1 \tag{2.6}$$

where H(k), W(k) are the Fourier transform of h(n) and w(n), respectively. It is noted that the relationship between the transmitted signal and received signal for a UWA channel can be clearly expressed by means of H(k) and W(k) in the frequency-domain.

The compensated signal after channel estimation is congregated into a serial sequence, which is then demodulated and decoded by the corresponding methods in the transmitter. At this point, the output of UWA-OFDM system model is obtained as the final binary data sequence.

2.2 CHANNEL ESTIMATION

The aim of channel estimation is to estimate channel parameters from the received signal. As discussed in (2.6), each subcarrier component of the received signal can be expressed as the product of the transmitted signal and channel frequency response at the subcarrier as long as no inter-carrier interference (ICI) occurs. Thus, the transmitted signal can be recovered by estimating the channel response at each subcarrier. In general, channel estimation is executed with the help of pilot symbols, which are known to both transmitter and receiver. As shown in Fig. 2, the pilot symbols can be inserted into the frequency or time direction in OFDM frames, namely comb-type and block-type, respectively. After obtaining the state estimation at the pilot symbols, the channel responses of all subcarriers between pilot symbols can be estimated by employing various interpolation methods, such as linear interpolation, second-order interpolation, spline cubic interpolation.

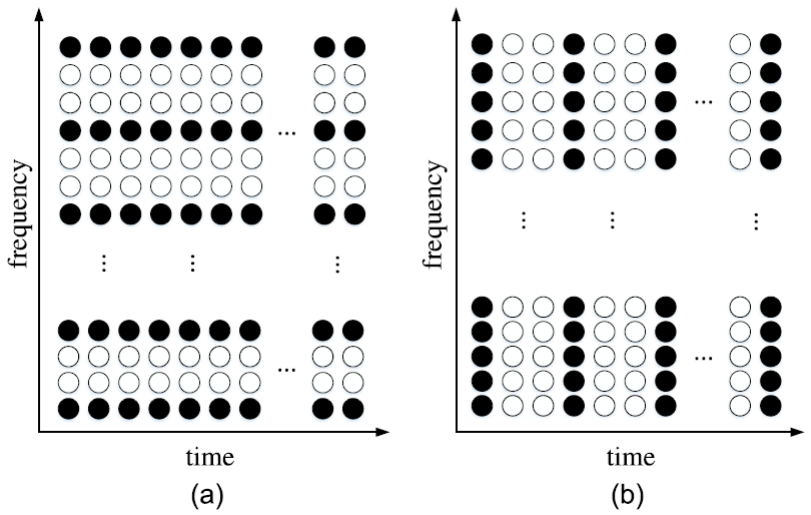

Figure 2.2: Two different types of pilot structures for UWA-OFDM systems.

LS algorithm is the most typical representative of the traditional channel estimation method, essentially to solve a problem of extreme value. Assuming the estimated channel impulse response is $\hat{H}_{LS}$, LS algorithm gives the solution to channel estimation for UWA-OFDM systems as follows:

$$\hat{H}_{LS} = (X^H X)^{-1} X^H Y = X^{-1} Y \tag{2.7}$$

where the superscript $(.)^H$ stands for the Hermitian transpose. It denotes that LS channel estimator is directly obtained by minimizing the square distance between the received symbols Y and the transmitted symbols X. Therefore, it is widely used for channel estimation due to its simplicity and without channel statistics required. However, it neglects the noise interference in the calculation process, resulting poor performance in complex UWA communication environment. To overcome the noise-sensitive defects of LS algorithm, MMSE algorithm is calculated based on minimizing the mean square error (MSE) of the actual channel and its estimation. Combined with the LS channel estimation result $\hat{H}_{LS}$ in (2.7), the MMSE estimator can be achieved as follows:

$$\hat{H}_{MMSE} = R_{H\hat{H}}(R_{HH} + \frac{{\delta_n}^2}{{\delta_x}^2} I)^{-1} \hat{H}_{LS} \tag{2.8}$$

where $R_{HH} = E(HH^H)$ refers to the autocorrelation matrix of channel response in frequency domain, and RHH˜ denotes the cross-correlation matrix between the actual channel and temporary estimated channel.${\delta_n}^2$ and ${\delta_x}^2$ are the variance of AWGN and transmitted signal, respectively. The influence of noise is taken into account by MMSE algorithm to improve the channel estimation accuracy. However, it is more complex than the LS algorithm because it requires some prior knowledge about the channel statistical properties, including the channel autocorrelation matrix and noise variance.

2.3 Deep Neural Networks Architectures

This section describes the architectures of our proposed DNN-based methods and the methodology of their usage for channel estimation in UWA-OFDM systems.

2.3.1 Prelimnary

In this subsection, we will begin by describing the simplest neural network with only a single neuron, as shown in Fig.2.3.

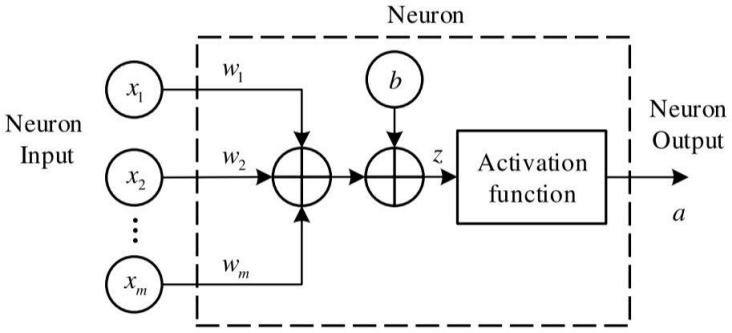

Figure 2.3: Inside structure of a neuron in the neural network. The neuron output is the calculation result of the inputs, weights, and a bias through an activation function.

The neuron is a computational unit related to the inputs,the weights for corresponding inputs,and the bias b used to model the threshold. In this figure, the weighted computation z can be adopted as:

$$z = \sum_{i=1}^{m} w_i x_i + b \tag{2.9}$$

The output of the neuron, denoted by a, is the result of a linear or nonlinear transformation of variable z, as follows:

$$a = f(z) = f(\sum_{i=1}^{m} w_i x_i + b) \tag{2.10}$$

where f() is called the activation function. By introducing nonlinear factors into the neuron, the activation function translates the input signal to the output signal so that the neural network can approximate any nonlinear function arbitrarily. Different activation functions and their variants have been proposed in various neural networks over the years. Among them, the most commonly used activation functions, sigmoid, hyperbolic tangent (tanh), linear, and rectified linear unit (ReLU) functions.

Fig.2.4 plots these four activation functions. Note that the sigmoid function squashes the real numbers to a different dynamic interval of [0, 1], while the hyperbolic tangent (tanh) function squashes to [1, 1]. The ReLU function is a halfwave rectifier and it saturates at exactly 0 whenever the input z is less than 0. Unlike these three, the linear function does not condense the network input so that it

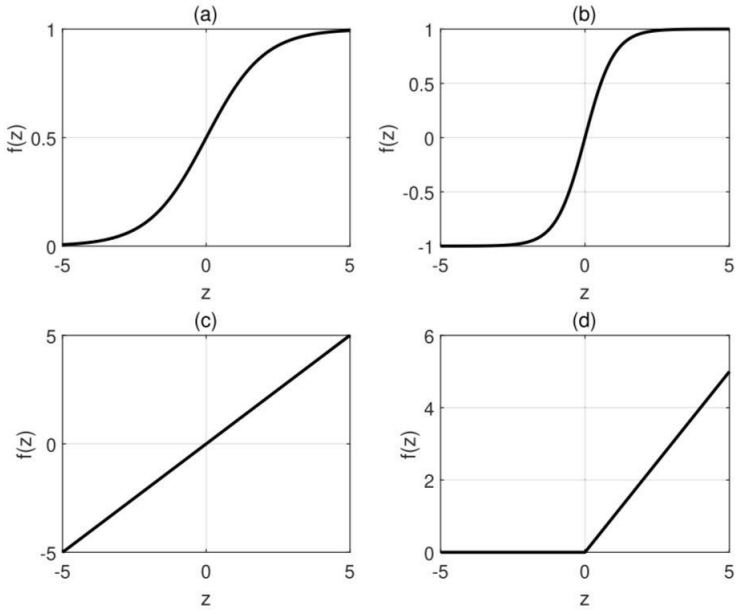

Figure 2.4: Commonly used activation functions in neural networks. (a) Sigmoid function. (b) hyperbolic tangent function (tanh). (c) linear function (here, c = 1, d = 0). (d) ReLU function.

2.3.2 Network Architectures

A neural network is usually comprised of numerous neurons as described in Fig.2.3, which are fully interconnected to each other to form a grid. There is a weight factor between every two neurons in different adjacent layers and these weights are dynamically adjusted during the training process. This configuration makes the output of a neuron in the anterior layer can be the input of another neurons in the latter layer. A standard three-layer neural network is embedded in the leftmost layer of the network is called the input layer, and the rightmost layer the output layer. The middle layer between the input layer and the output layer is called the hidden layers because their values are invisible in the training process. It is well known that DNN inherits from the classical neural network but includes more hidden layers and more neurons. Its deep architecture promotes the model to yield better performance in very complex and highly nonlinear problems than the traditional methods. Hence in this paper, the DNN model, as illustrated in Fig.2.5, is introduced to estimate the channel coefficients in UWA-OFDM systems since this approach is applicable in channel estimation problems for its outstanding learning, representation, and approximation ability.

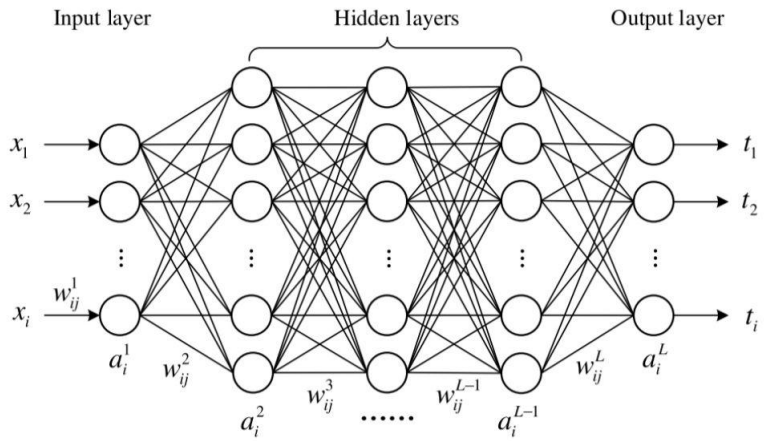

Figure 2.5: Typical architecture of deep neural network model. It consists of an input layer, multiple hidden layers, and an output layer. The neurons in the two adjacent layers are fully connected, whereas the neurons in each layer are not connected.

2.3.3 Model Training

In general, the deployment of DNN model contains two stages, the training process and the working process. Before implemented to estimate the channel parameters effectively in the working process, the network model must be trained by training symbols in the training process.

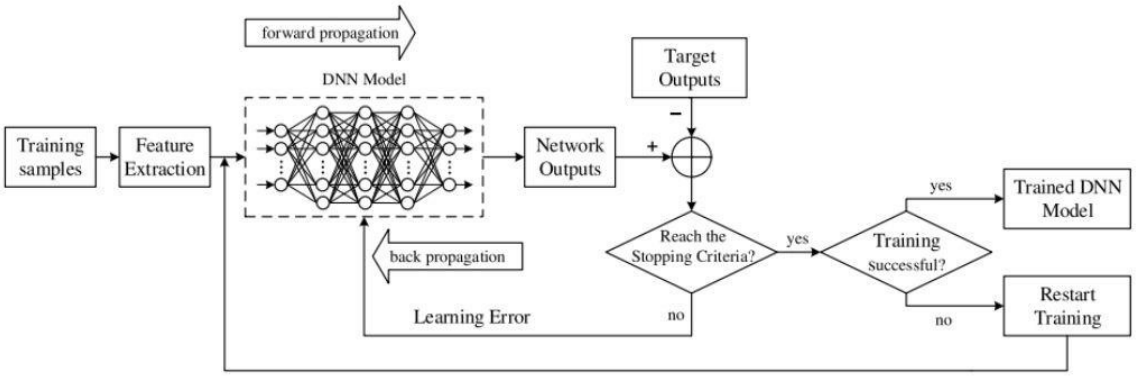

Figure 2.6: Training process of the proposed DNN models. The objective of training a DNN is to find the optimal parameters of weights and biases to minimise the error between the network outputs and the target outputs.

The training process of DNN model can be summed up as the forward propagation of the training symbols and the back propagation of the learning error, as presented in Fig.2.6 Originally, the training input data are dealt by the neurons in hidden layers and then are transmitted to the output layer. If the results of the output layer do not match the desired ones, the learning errors between the network outputs and target outputs will be backtracked from the output layer to hidden layers. Meanwhile, the weights and biases in the neurons will be modified according to the learning errors respectively. The training process will be repeated until the stopping criteria are reached, such as a given number of iterations have been completed, or a chosen goal of the learning error has been satisfied, etc. In this paper, two DNN models, labeled by DNN-1 and DNN-2, are proposed for channel estimation with five layers, consisting of an input layer, three hidden layers and an output layer.

Layer	**BPNN** [31]		**DNN-1**[ours]		**DNN-2**[ours]	
	Nodes	$f(\cdot)$	Nodes	$f(\cdot)$	Nodes	$f(\cdot)$
Input	2	–	4	–	16	–
Hidden #1	10	tanh	32	tanh	64	tanh
Hidden #2	–	–	32	tanh	64	tanh
Hidden #3	–	–	32	tanh	64	tanh
Output	2	linear	4	linear	16	linear

Simulation parameters of the UWA-OFDM system.

Parameter	**Value**
Number of subcarriers	1024
FFT size	1024
Type of modulation	16, 32, 64QAM
Type of pilot insertion	Comb
Type of guard interval	Cyclic prefix
Length of guard interval	256
Channel model	UWA multipath channels
Noise model	Additive White Gaussian Noise

Training parameters of neural network models.

Figure 2.7

As presented in Table above, the numbers of neurons in each layer are 4, 32, 32, 32, 4 in DNN-1 and 16, 64, 64, 64, 16 in DNN-2, respectively. These parameters of designed layers and neurons are obtained with iterative simulations. To adopt the UWA-OFDM signal to neural network, the complex signal is separated into real and imaginary parts, since neural network allows only the real format whereas the UWA-OFDM signal is in complex format. In our proposed channel estimator, the DNN models are firstly trained before deployment with the training received pilot symbols and the correct channel impulse responses in the training process. Every two pilot symbols and every eight pilot symbols are grouped into the models of DNN-1 and DNN-2 respectively, then the corresponding outputs of each DNN model are gathered together for the final outputs. Hyperbolic tangent function is chosen as the activation function in hidden layers and linear function is chosen in output layer, for both of these network models. Besides, 1,318,400 training samples, randomly divided into 70% as training set, 15% as test set, and 15% as validation set, are utilized to train the each considered type of neural network. Finally, in the working process, the current received pilot symbols are fed into the trained DNN models and the outputs of the networks will be the estimated channel impulse responses. The detailed procedure of DNN-based channel estimation is exhibited in Algorithm 1.

2.3.4 Bellhop Ray Tracing

Modeling acoustic propagation conditions is an important issue in underwater acoustics and there exist several mathematical/numerical models based on different approaches. Some of the most used approaches are based on ray theory, modal expansion and wave number integration techniques. Ray acoustics and ray tracing techniques are the most intuitive and often the simplest means for modeling sound propagation in the sea. Ray acoustics is based on the assumption that sound propagates along rays that are normal to wave fronts, the surfaces of constant phase of the acoustic waves. When generated from a point source in a medium with constant sound speed, the wave fronts form surfaces that are concentric circles, and the sound follows straight line paths that radiate out from the sound source. If the speed of sound is not constant, the rays follow curved paths rather than straight ones. The computational technique known as ray tracing is a method used to calculate the trajectories of the ray paths of sound from the source. Ray theory is derived from the wave equation when some simplifying assumptions are introduced and the method is essentially a high-frequency approximation. The method is sufficiently accurate for applications involving echo sounders, sonar, and communications systems for short and medium short distances. These devices normally use frequencies that satisfy the high frequency conditions.

However,ray theory has limitations and may not be valid for precise predictions of sound levels, especially in situations where refraction effects and focusing of sound are important. There exist corrective measures that can be used to improve classical ray theory. A number of realistic examples and cases are presented with the objective to describe some of the most important aspects of sound propagation in the oceans. This includes the effects of geographical and oceanographic seasonal changes and how the geoacoustic properties of the sea bottom may limit the propagation ranges, especially at low frequencies. The examples are based on experience from modeling sonar systems, underwater acoustic communication links and propagation of low frequency noise in the oceans. There exist a number of ray trace models, some are tuned to specific applications, and others are more general.

Eigenray determination

To calculate the acoustic field it is necessary to have an efficient and accurate algorithm for determination of eigenrays. An eigenray is defined as a ray that connects a source position with a receiver position. In most case with multipath propagation there are many eigenrays for a given source/receiver configuration, which means that finding all eigenrays is not a trivial task. The PlaneRay model uses a unique sorting and interpolation routine for efficient determination of a large number of eigenrays in range dependent environments. This approach is described by the two plots in Figure 6, which displays the ray history as function of initial angle at the source. All facts and features of the acoustic fields such as the transmission loss, transfer function and time responses are derived from the ray traces and their history The two plots show the ranges and travel times to where the rays cross the receiver depth line . A particular ray may intersect the receiver depth line, at several ranges. For instance at the range of 2 km, there are 11 eigenrays and from Figure 6 the initial angles of these rays are approximately found to be 5.9,9.6,22,24 degrees for the positive (down going) rays and 2.0,3.6,7.4,15.0 17.0,25,27.0 degrees for the negative (up-going waves). However, the values found in this way are often not sufficiently accurate for the determination of the sound field.

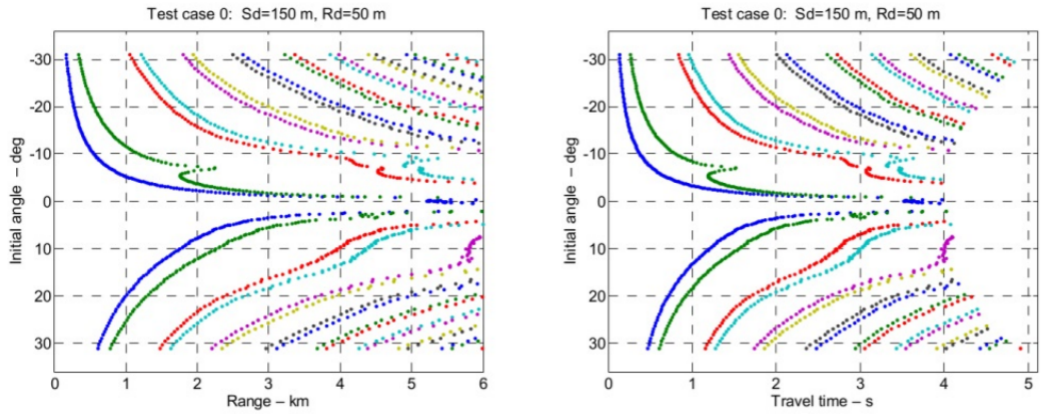

Figure 2.8

Further processing may therefore be required to obtain accurate results. The graphs of Figure 2.8 are composed of independent points, but it is evident that the points are clustered in independent clusters or groups. This property is used for sorting the points into branches of curves that represents different ray history. These branches are in most case relatively continuous and therefore amenable to interpolation. An additional ad-

vantage of this method is that the contribution of the various multipath arrivals can be evaluated separately, thereby enabling the user to study the structure of the field in detail.

In most cases the eigenrays are determined by one simple interpolation yields values that are sufficiently accurate for most application, but the accuracy increases with increasing density of the initial angles at the cost of longer computation times. Figure 7 shows examples of eigenrays traces with rays a receiver located at 2.5 km from the source for the scenario shown in Figure 2.9. To this receiver there are a total of 12 eigenrays, spanning the range of initial angles from -30 to 29 degrees.

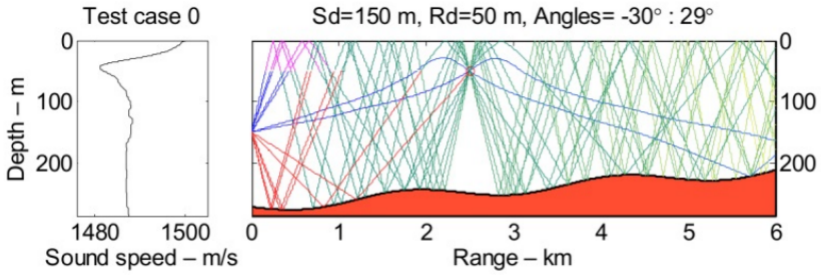

Figure 2.9

2.3.5 Analysis

To demonstrate the performance of our proposed DNN models for channel estimation, experiments have been carried out to compare with the conventional LS algorithm [13], MMSE algorithm [13] and BPNN [30] in terms of BER and NMSE versus SNR criteria. The parameters of the UWAOFDM system and neural network training used in our simulations are given in Table. 2 and Table. 3, respectively. Additionally, to increase the reliability and accuracy of our experiments, we utilize the BELLHOP ray model to simulate the UWA communication environment in this paper.

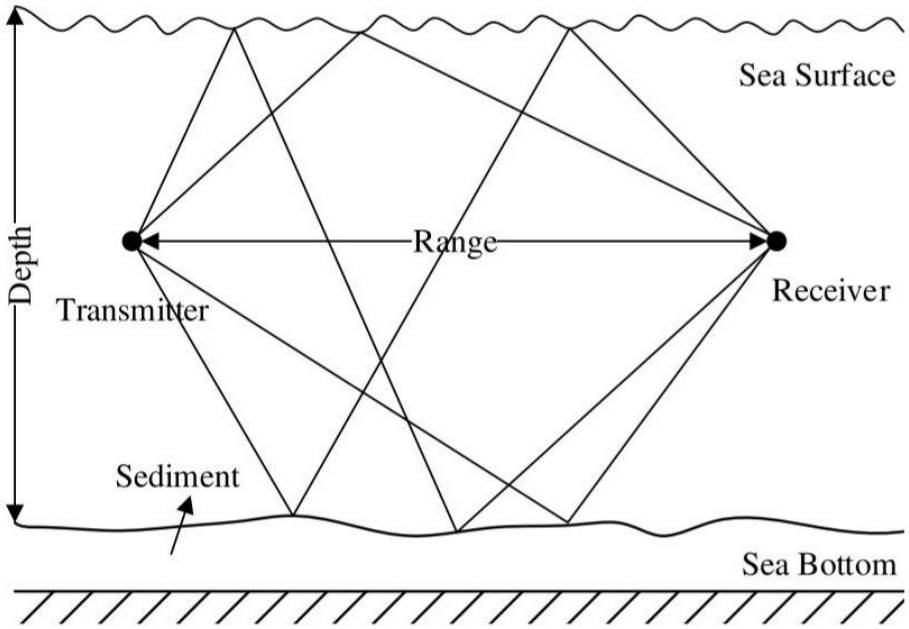

Figure 2.10: BELLHOP ray model of a shallow UWA multipath channel. It takes into account environmental factors including the variation of sound speed at depths, shapes of sea surface and bottom, boundary reflection and scattering, and geometry of the transmitter and receiver.

As illustrated in Fig.2.8, the BELLHOP ray model is used to predict acoustic wave propagation in water columns with consideration of sound speed profile (SSP), boundaries of sea surface and sea bottom, reflection and scattering in boundaries, and geometry of the transmitter and receiver. The depth of water column is 100 m and the range between transmitter and receiver is approximately 1000 m. As expressed to be a function of temperature, salinity and depth, the sound speed increases from 1537 m/s at the surface of the water column to 1540 m/s at the bottom. In the sediment layer, the sound speed is 1650 m/s and the attenuation coefficient is 0.8 dB/. The density of water is 1.0 g/cm3 and

that of the sediment layer is 1.9 g/cm3 . Based on the schematic diagram of BELLHOP ray model in Fig.2.8, two different UWA multipath channels with three taps and seven taps are modeled to investigate the performance of UWA-OFDM systems, labeled by channel-I and channel-II, respectively.

Simulated diagrams after using Bellhop Ray Model

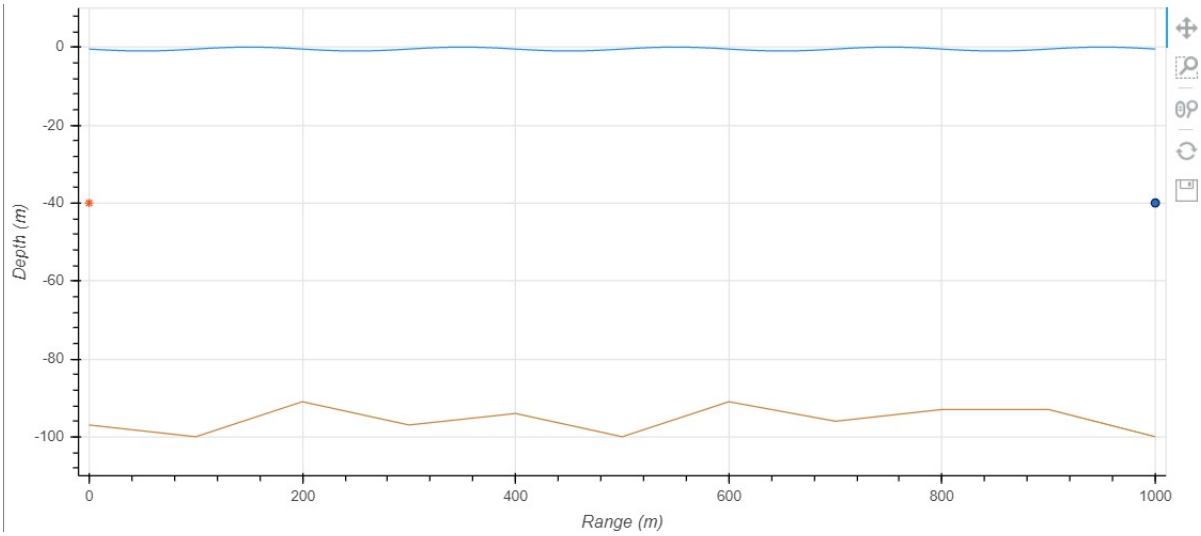

Figure 2.11: Assumed Underwater Environment Model

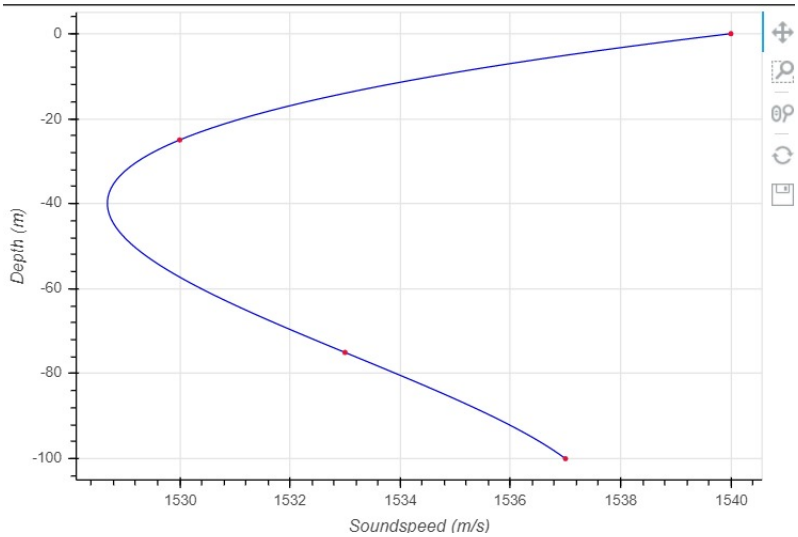

Figure 2.12: Sound Diagram

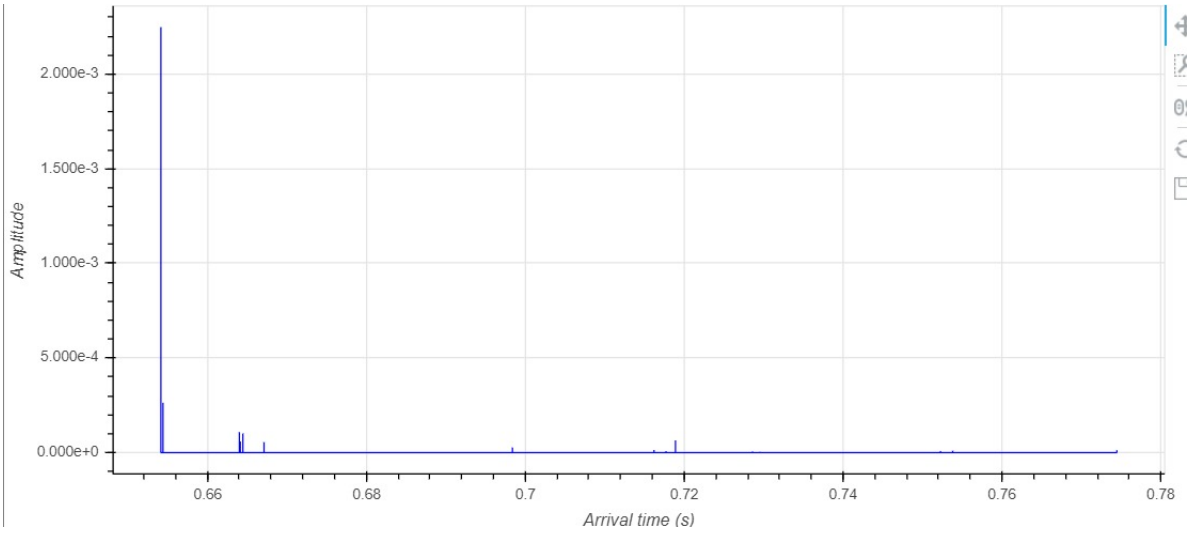

Figure 2.13: Impulse Response Showing Arrival time

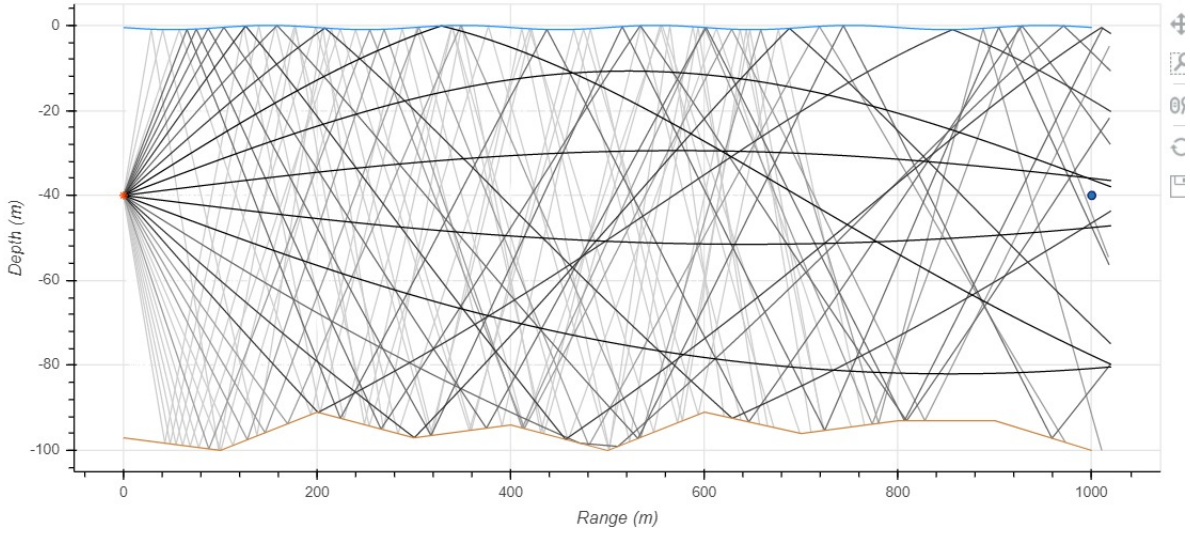

Figure 2.14: Computed Race Diagram

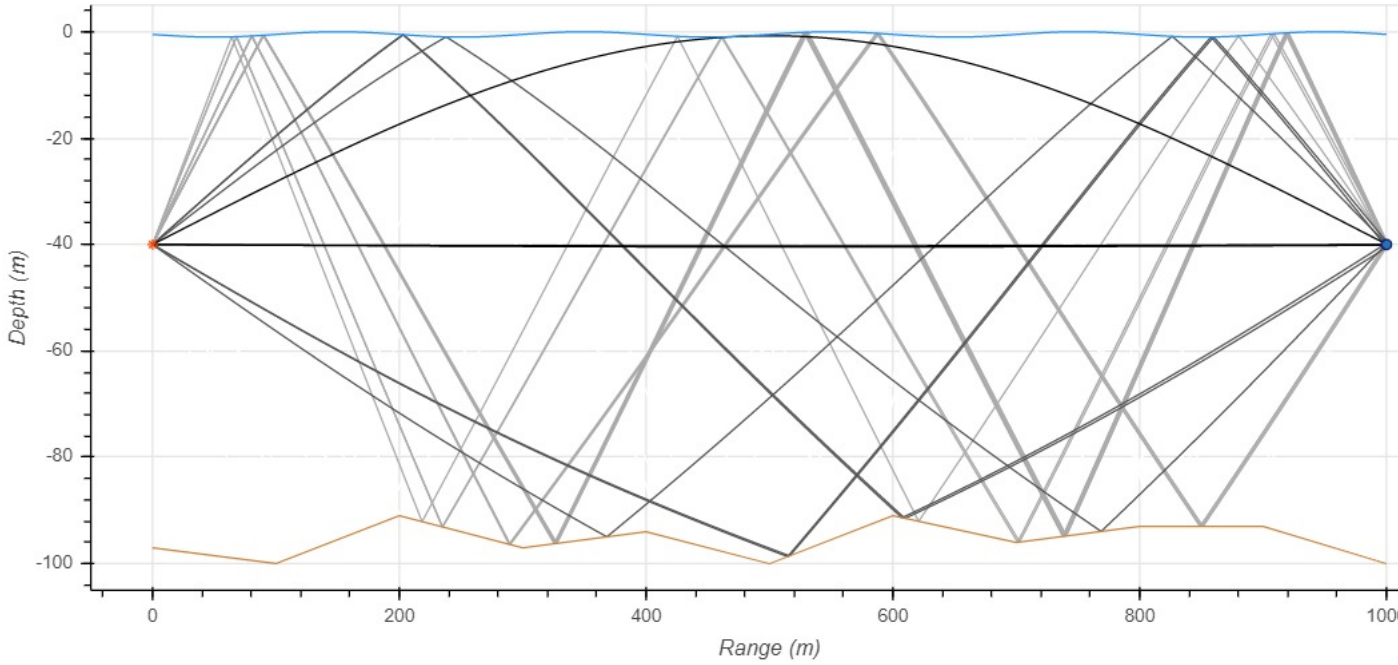

Figure 2.15: Eigen Rays Diagram

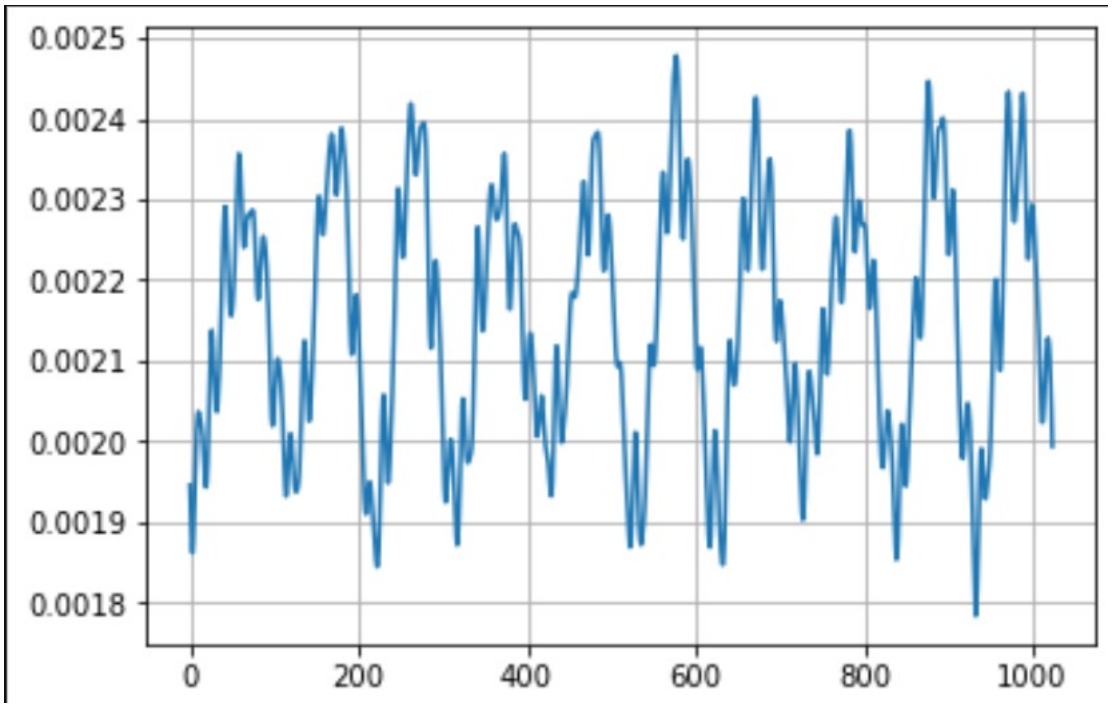

Figure 2.16: Impulse Response in Frequency domain

CHAPTER 3

Conclusions

We have designed our project till developing OFDMI system and channel estimation using Least Square Method and Mmse Method,the follwing results are as shown in this section.

3.1 Analysis

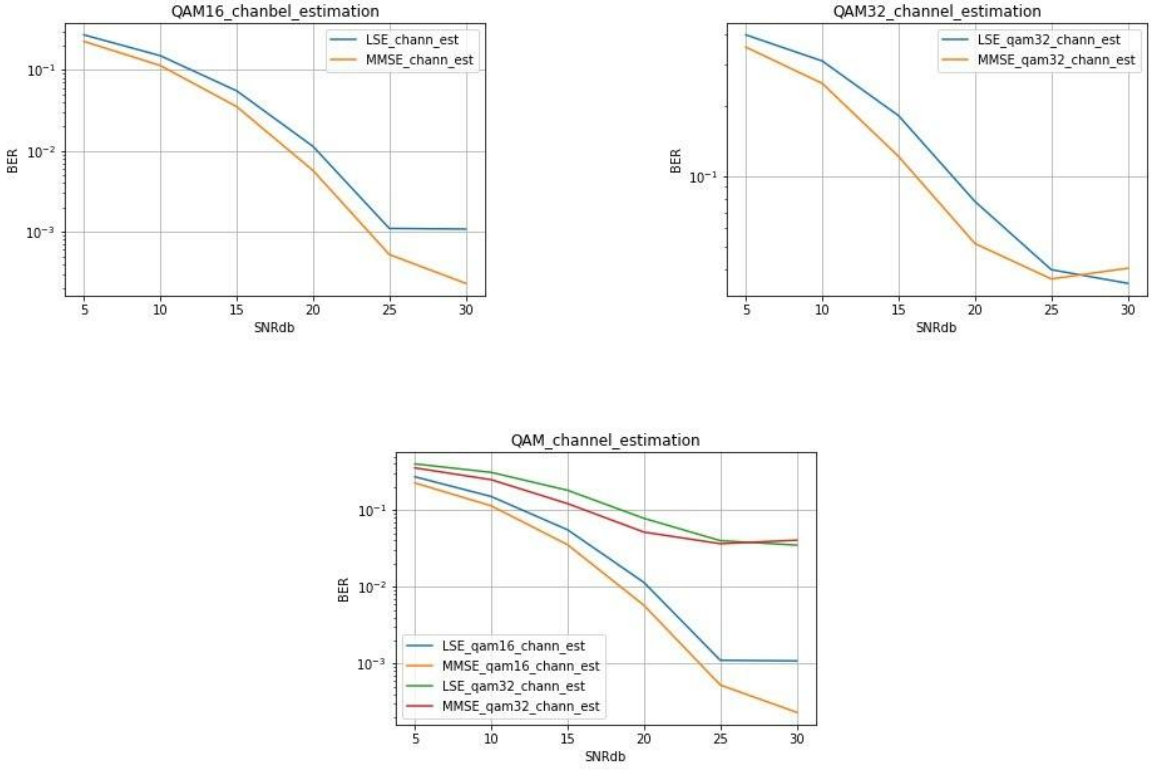

Figure 3.1: QAM - Channel Estimation Graphs

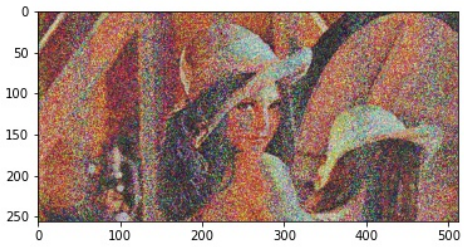

QAM 16 ls SNR 5db

QAM 16 ls SNR 10db

QAM 16 ls SNR 15db

QAM 16 ls SNR 20db

QAM 16 ls SNR 25db

QAM 16 ls SNR 30db

Figure 3.2: QAM-16 of LS Method for different SNR values

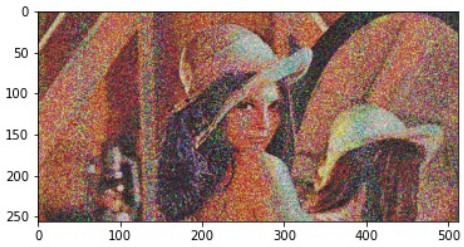

QAM 16 mmse SNR 5db

QAM 16 mmse SNR 10db

QAM 16 mmse SNR 15db

QAM 16 mmse SNR 20db

QAM 16 mmse SNR 25db

QAM 16 mmse SNR 30db

Figure 3.3: QAM-16 of MMSE Method for different SNR values

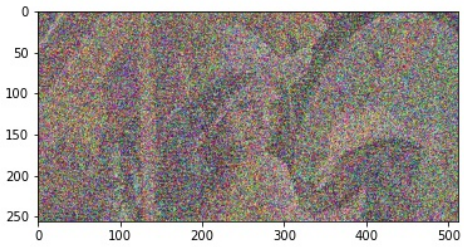

QAM 32 ls SNR 5db

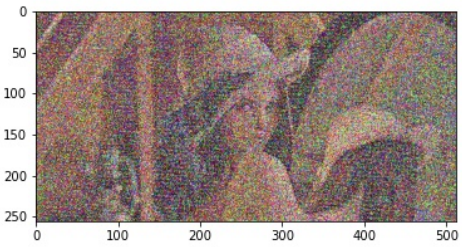

QAM 32 ls SNR 10db

QAM 32 ls SNR 15db

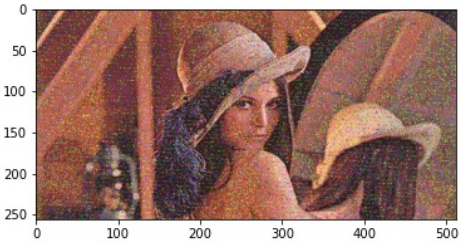

QAM 32 ls SNR 20db

QAM 32 ls SNR 25db

QAM 32 ls SNR 30db

Figure 3.4: QAM-32 of LS Method for different SNR values

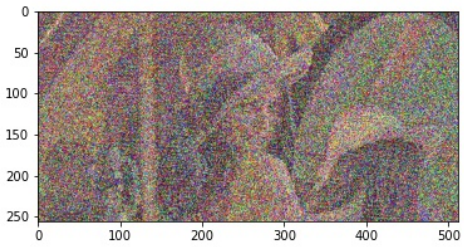

QAM 32 mmse SNR 5db

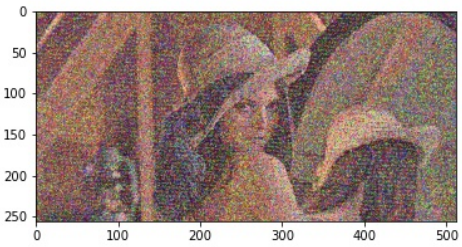

QAM 32 mmse SNR 10db

QAM 32 mmse SNR 15db

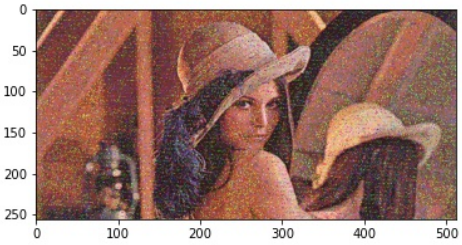

QAM 32 mmse SNR 20db

QAM 32 mmse SNR 25db

QAM 32 mmse SNR 30db

Figure 3.5: QAM-32 of MMSE Method for different SNR values

3.2 Future Work

- In the coming days we are planning to work on different modulation techniques other than QAM.
- We are planning to develop CNN,Encoding Architectures for deep neural networks other than fully connected layers.

REFERENCES

[1] J. Preisig, "Acoustic propagation considerations for underwater acoustic communications network development," ACM SIGMOBILE Mobile Comput. Commun. Rev., vol. 11, no. 4, pp. 2–10, Oct. 2007.

[2] M. Stojanovic and J. Preisig, "Underwater acoustic communication channels: Propagation models and statistical characterization," IEEE Commun. Mag., vol. 47, no. 1, pp. 84–89, Jan. 2009.

[3] R. Diamant and L. Lampe, "Low probability of detection for underwater acoustic communication: A review," IEEE Access, vol. 6, pp. 19099–19112, 2018.

[4] G. Qiao, Z. Babar, L. Ma, S. Liu, and J. Wu, "MIMO-OFDM underwater acoustic communication systems—A review," Phys. Commun., vol. 23, pp. 56–64, Jun. 2017.

[5] T. Lufen and X. Xu, Digital Underwater Acoustic Communications, 1st ed. New York, NY, USA: Academic, 2017.

[6] R. Jiang, S. Cao, C. Xue, and L. Tang, "Modeling and analyzing of underwater acoustic channels with curvilinear boundaries in shallow ocean," in Proc. IEEE Int. Conf. Signal Process., Commun. Comput. (ICSPCC), Oct. 2017, pp. 1–6.

[7] P. C. Etter, Underwater Acoustic Modeling and Simulation. Boca Raton, FL, USA: CRC Press, 2018.

[8] R. Prasad, OFDM for Wireless Communications Systems. Norwood, MA, USA: Artech House, 2004.

[9] B. Li, S. Zhou, M. Stojanovic, L. Freitag, and P. Willett, "Multicarrier communication over underwater acoustic channels with nonuniform Doppler shifts," IEEE J. Ocean. Eng., vol. 33, no. 2, pp. 198–209, Apr. 2008.

[10] P. Vimala and G. Yamuna, "Pilot design strategies for block sparse channel estimation in OFDM systems," Indian J. Sci. Technol., vol. 10, no. 24, pp. 1–6, 2017.